

# Investigation of performance of free-piston engine generator with variable-scavenging-timing technology under unsteady operation condition

## Abstract

A substantial number of free-piston engine generators still use cross scavenging, which limits scavenging quality and performance under unsteady condition. Variable-scavenging-timing technology is a novel method to change the fixed scavenging process so that the scavenging process is coordinated with piston movement. This paper investigated effects of the variable-scavenging-timing technology implemented on the free-piston engine generator. In designed case that the free-piston engine generator has different compression ratios, cyclic variation and frequency, the variable-scavenging-timing technology improved the scavenging quality and performance. The delivery ratio of the free-piston engine generators applied with the variable-scavenging-timing technology decreased about 0.3 at different compression ratios, 0.18 at different cyclic variations and 0.2 at different frequencies on average. The trapping efficiency of FPEG rose over 70 % and the scavenging efficiency was maintained at least 85 %. As for different compression ratios, the power increased by an average of 0.18 kW. While the power was improved 0.2 kW on average under the other condition. The increase of indicated efficiency had an increase varying from 1 % to 2 % compared with before. The changes of the performance about free-piston engine generators under different unsteady condition also were discussed.

**Key words:** free-piston engine generators; scavenging efficiency and performance; variable-scavenging-timing technology; compression ratio; frequency; cyclic variation

## 1 Introduction

### 1.1 Background

In order to cope with climate warming and excessive energy exploitation, people are more inclined to seek new environmentally friendly power plants with better performance. Since the technology of four-stroke internal combustion has encountered

31 kinds of bottlenecks, two-stroke internal combustion became one of the research  
32 objectives for its potential indicated performance and efficiency, and thus attracted  
33 more and more attention. However, it is not as precise and sophisticated as four-stroke  
34 combustion engine. In order to overcome the inherent shortcomings of two-stroke  
35 internal combustion engine, the free-piston engine generator (FPEG) thus emerged [1].

36 FPEG consists of two free-piston engines and a linear alternator, with variable  
37 compression ratio, compact structure and other characteristics [2]. Compared with  
38 traditional two-stroke combustion, it requires less mechanical compartments and is  
39 driven by linear piston force, which helps reduce overall complexity and facilitates the  
40 use of algorithmic control, resulting in better device maneuverability and less  
41 mechanical loss. Variable compression ratios help improve efficiency and realize the  
42 potential to meet a wide range of power requirements [3]. In addition, FPEG has  
43 potential applications as a range extender for hybrid electric vehicles, which gives it the  
44 ability to convert electrical energy and kinetic energy.

45 Due to the characteristics of the FPEG, it is believed that FPEG should be  
46 popularized to ensure its stable operation [4]. Combustion is a dynamic response. For  
47 example, if its compression changes, its piston motion must become inconsistent.  
48 Optimal ignition timing and other factors need to be adjusted. On the basis of  
49 maintaining the continuous operation of FPEG, it is proposed to transform the internal  
50 structure and external combination of new technology[5]. For the sake of internal  
51 integrity, one attempt is to optimize intrinsic scavenging using new methods. It is  
52 suggested that scavenging is matched with piston displacement to create a suitable  
53 environment for the generation and scavenging of internal combustion engine. In this  
54 paper, it is identified as variable-scavenging-timing technology. The variable-  
55 scavenging-timing technology is to provide appropriate scavenging mode for different  
56 operating modes of free-piston, which means scavenging serves good performance and  
57 is not limited to structure. In recent years, many researchers studying the FPEG seem  
58 to be focused on improving efficiency and performance. They built different simulation  
59 models and ran some experiments on their prototypes around the world. However,  
60 problems about scavenging are rarely focused as a key issue, and there is a phenomenon  
61 that study on new scavenging technology to be shelved after failing to the extent of the  
62 exploration. There are inadequate cases about the free-piston engine generator with new  
63 scavenging method.

**Nomenclature table**

BMEP	Brake mean effective power
ATDC	after top dead center
BTDC	before top dead center
$\epsilon$	compression ratio
CA	crank angle
Var	variation (mm)

VST	Variable-scavenging-timing
$m$	mass of the left piston(kg)
$F_l$	the in-cylinder gas force from the left cylinder (N)
$F_r$	the in-cylinder gas force from the right cylinder (N)
$F_f$	the frictional force the assembly of the piston (N)
$F_g$	the resistance force from linear electric motor (N)
$C_f$	the viscosity friction coefficient (N/(m·s <sup>-1</sup> ))
$K_v$	the coefficient of electromagnetic resistance (N/(m·s <sup>-1</sup> ))
$v$	the velocity of the piston (m/s)
$\eta_s$	the scavenging efficiency
$\eta_t$	the delivery ratio
$\eta_{te}$	the trapping efficiency
$\dot{m}$	the instantaneous air flow (kg/s)
$m_0$	the mass of fresh air trapped in the cylinder(kg)
$m_r$	the mass of the exhaust gas trapped in the cylinder (kg)
$m_t$	the mass of the intake air (kg)
$m_{sv}$	The mass required to fill the swept volume (kg)
$\rho$	gas density at the inlet manifold (kg/m <sup>3</sup> )
$v_m$	the total average flow velocity at the port (m/s)
$n$	the engine speed of the FPEG (rpm)
$\phi$	The angle of the air port (CA°)
$A_f$	the instantaneous cross section area of air flow (m <sup>2</sup> )
$x_b$	the mass fraction burned
$t_0$	the beginning of the combustion (CA°)
$\Delta t$	the duration of the combustion (CA°)
$a$	Vibe coefficients
$m$	Vibe coefficients
$h_c$	heat transfer coefficient
$B$	the characteristic length of the bore (m)
$p_c$	the cylinder pressure (Pa)
$T_c$	The cylinder temperature (K)
$C$	empirical parameters
$\eta$	empirical parameters
$\omega$	the gas velocity (m/s)
$\eta_i$	the indicated efficiency
$b_i$	the fuel consumption per hour (g/(kW·h))
$H_u$	the low heating value of the fuel (MJ/Kg)

$P_b$	brake power of the free-piston engine (kW)
$L$	the piston stroke (m)
$A$	the area of the piston head (m <sup>2</sup> )
$V_s$	the sweeping volume (m <sup>3</sup> )
$\bar{p}_b$	the brake mean effective pressure (MPa)

65 *1.2 Literature review*

66 In the 1920s, the study of free-piston engine began to appear, and Pescara put  
67 forward the numerical free-piston internal combustion engine model [6]. Since 1930,  
68 different types of free-piston engine have emerged. However, due to the slow  
69 development and many technical bottlenecks in the early stage, it was difficult for  
70 formal industrial products to appear before the public. At that time, free-piston engines  
71 were used as air compressors and gas generators to complement conventional internal  
72 combustion engines and gas turbines [7]. It can be classified as symmetric and  
73 asymmetric. In addition to diesel, it can also be used as fuels such as heavy oil, crude  
74 oil and natural gas.

75 Researchers from West Virginia University have proposed a spark-ignited free-  
76 piston linear engine that reports achieving a cylinder diameter of 36.5 mm and a  
77 maximum stroke of 50 mm in continuous operation [8-10]. They also simulated the  
78 motion characteristics and other performance parameters of the piston by combining  
79 experimental data with basic theory. However, in the absence of an active control  
80 method for the electromagnetic force and piston motion to regulate its operating  
81 conditions, the FPLE ultimately produced a power output of 316 W and energy  
82 efficiency of 11 % in converting fuel to electricity.

83 Mikalsen and Roskilly studied a numerical model of a single-cylinder FPLA  
84 generated by spark ignition [11, 12]. They developed a series of theories about the  
85 effects of piston motion, compression ratio, scavenging system and approaches of  
86 ignition functioning on the combustion [13, 14]. Jia et al. proposed a new approach of  
87 using cascade control to help the machine maintain stable operation [15-17]. Based on  
88 the accumulated experience, Ugochukwu Ngwaka et al. analyzed the parameters of a  
89 semi-closed-loop linear joule engine generator using argon and oxy-hydrogen  
90 combustion [18]. They found that extending the exhaust time of the expander could  
91 improve system efficiency and power output. It is suggested that free-piston engines  
92 should pay attention to scavenging.

93 Bergman and Fredriksson et al. presented a CFD of two-stroke free-piston  
94 converter with single-flow scavenging [19]. They studied the performance of the single-  
95 flow scavenging under the conventional and HCCI (Homogeneous Charge  
96 Compression Ignition) modes [20]. In order to avoid complicated calculation, the piston  
97 motion is fixed. This method was further used in the subsequent simulations or  
98 experiments, in which ignition timing was changed to achieve different results. The  
99 results showed that under the traditional mode, low compression ratio led to low

100 emission. And Blarigan et al. from Sandia National Laboratories developed an  
101 optimized scavenging system using Kiva-3V computational fluid dynamics (CFD) code  
102 and a zero-dimensional piston dynamics model to improve power, economy, and  
103 emission performance[21]. In addition to the scavenging performance, the design  
104 schemes of circulation, various charge delivery options and single flow scavenging  
105 were also discussed. The results showed that the single-flow scavenging system had a  
106 constant and low value of thermal charging environment.

107 Sofianopoulos et al., at Stony Brook University conducted experiments on the  
108 scavenging process and found that in the early stages of the scavenging process, fresh  
109 charge with low momentum ran into the exhaust passage, reducing trapping efficiency  
110 [22]. The fresh charge with high momentum brought into the combustion chamber and  
111 exhaust gas produced in the final stage of scavenging affected the cycle loss. The  
112 residual combustion waste in scavenging port would reduce scavenging efficiency.  
113 Although the boosting pressure might improve the scavenging efficiency, the initial  
114 cycle loss was bound to increase, leading to a decrease in the trapping efficiency.  
115 Therefore, Lu et al. from Beijing Institute of Technology focused on the scavenging  
116 ports width to scavenging process based on the opposed-piston two-stroke engine and  
117 explore the limit of scavenging limit by adjusting the structure [23]. Their results  
118 indicated that the width of exhaust ports had a greater impact on the scavenging  
119 efficiency and that when load and speed increased, the timing of free exhaust would  
120 decrease while that of the scavenging process would increase.

121 In order to surge the diversity of researches on scavenging of free-piston, Yuan et  
122 al. used a coupling model to explore the difference between free-piston linear engine  
123 and conventional two-stroke engine [24, 25]. Compared with the conventional two-  
124 stroke engine, it has shorter scavenging period and greater movement speed [26].  
125 Therefore, the higher the speed, the more residual combustion wastes it would produce.  
126 The faster piston motion results in the loss of scavenging efficiency, with more residual  
127 gas coming from the cylinder. In addition, he also claimed that late ignition and long  
128 combustion duration are conducive to improve scavenging efficiency to the 96.82% at  
129 the highest and a little in-cylinder fresh charge [27]. Dong et al. studied the  
130 characteristics of gas consumption, which is scavenging flow through the valve per unit  
131 time in the reference. [28]. They believe that tail gas back pressure has a great influence  
132 on gas consumption, showing a trend of intersection between tail gas consumption  
133 curve representing high gas consumption and curve representing low gas consumption.  
134 In order to obtain the same mass flow, when the mass flow is lower than the crossing  
135 point, the lower the exhaust back pressure is, the lower the inlet compression ratio  
136 which means the ratio of scavenging pressure to exhaust pressure is. Above the crossing  
137 point, the lower the exhaust back pressure, the smaller the required intake compression  
138 ratio.

139 In addition, Mao and Feng et al. used a multi-dimensional CFD model to conduct  
140 a global study on the loop scavenging piston linear engine ignited by spark [29]. The  
141 simulation results showed that proper scavenging efficiency and trapping efficiency

142 required higher effective stroke to bore ratio, a larger disc overlapping angle and a low  
143 supercharge. Gibbes and Hong proposed a free-piston engine alternator with piston-  
144 mounted passive inlet poppet valve and its relative two-dimensional axis-symmetric  
145 CFD scavenging model [30]. Wang et al. from Tianjin University used a three-  
146 dimensional CFD model based on piston displacement to analyze the single-flow  
147 scavenging of opposed-piston and opposed-cylinder hydraulic free-piston engines [31].  
148 The simulation results showed that the radial angle of the inlet had an important effect  
149 on the scavenging performance, and that the effect of piston movement on the  
150 ventilation performance was also worth further study. Zhaoping Xu et al. proposed a  
151 prototype of a novel internal combustion linear generator integrated power system [32].  
152 It is found that variable intake stroke length can be used to achieve different power  
153 output, and thermal efficiency can be improved by increasing expansion stroke length  
154 when the compression ratio is fixed.

155 Ensuring the relative stability of the gas exchange process is very important to  
156 maintain the stability of the air-fuel ratio and has a fundamental impact on combustion.  
157 As far as the existing simulation and experiment are concerned, most of the literatures  
158 reflect the results and laws of fixed scavenging process and steady working condition.  
159 Due to the movement characteristics of the FPEG, unsteady working conditions will be  
160 encountered in the experiment. In recent years, scavenging under the unsteady  
161 operation conditions such as different compression ratios or cyclic variations have been  
162 paid attention in the research about FPEG. The way to improve the performance and  
163 scavenging efficiency of the FPEG by solving the problem of unstable working  
164 environment has not been widely studied at present. The fixed scavenging hardly meets  
165 the demand in this aspect and the new technology should be introduced.

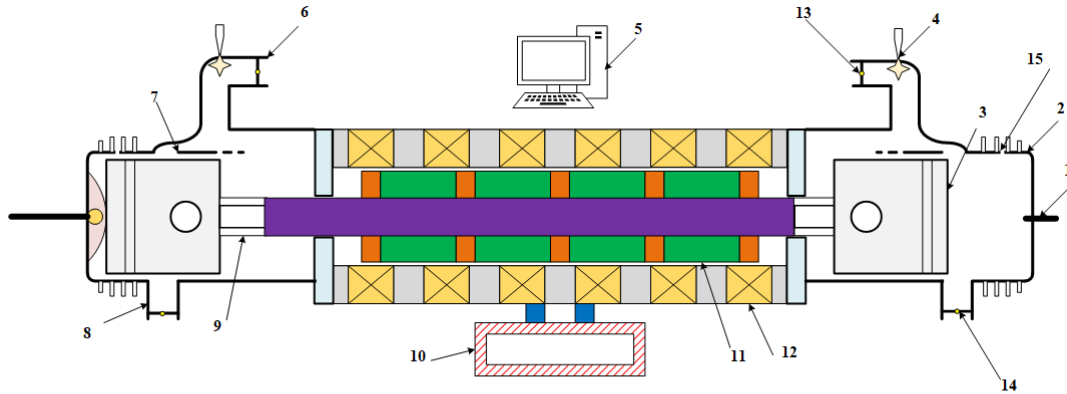
166 In this paper, a series of numerical simulations are carried out by using the control  
167 variable method, which responds to unsteady conditions by changing the scavenging  
168 process. By comparing the effect of conventional cross scavenging and variable-  
169 scavenging-timing technology on the performance and scavenging efficiency of the  
170 FPEG, some suggestions for improving the scavenging method are proposed. Specific  
171 results and discussion are described in the further section.

## 173 **2 System configuration and problem description**

### 174 *2.1 FPEG configuration*

175 The FPEG (schematic diagram is shown in Fig.1, with the corresponding  
176 prototype designed in the authors' group) is designed as a dual-cylinder, dual-piston  
177 engine with two-stroke thermodynamic cycle that it uses spark ignition instead of  
178 compression ignition [33]. Two opposing free-piston engines are combined with a  
179 linear motor located between the two cylinders. In addition, FPEG has the

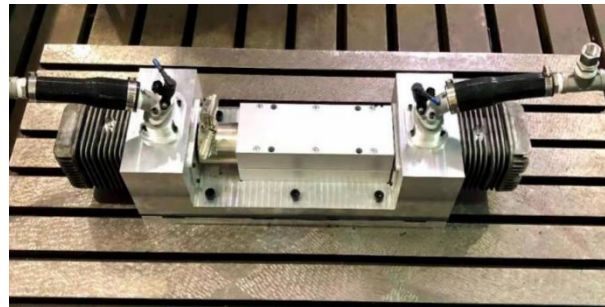
180 characteristics of compact structure and high power to weight ratio. The important  
 181 moving parts of the system are the two pistons connected with the engine of the linear  
 182 generator. The control system is adopted to ensure the stable operation of FPEG.  
 183 Compared with an internal combustion engine using a conventional crankshaft linkage  
 184 mechanism, FPEG has fewer components, which makes it easier to assemble and  
 185 significantly more mechanically efficient.



1. Spark plug 2. Cylinder 3. Piston 4. Fuel injector 5. Control system 6. Air-intake tube 7. Scavenging port 8. Exhaust port  
 9. The connecting rod 10. External load 11. Mover 12. Stator 13. Intake valve 14. Exhaust valve 15. Lubrication oil hole

186  
 187

**Fig. 1** Prototype schematic figure



188  
 189

**Fig. 2** Prototype figure

190 For the air port scavenging type, the opening/closing of the air port is determined  
 191 by the movement of the piston, and the timing is determined by the displacement of the  
 192 piston. The FPEG prototype designed by the author's group adopts cross-scavenging  
 193 type, that is, the inlet and exhaust ports are not on the same side. This scavenging  
 194 method mainly uses the pressure difference to sweep up the exhaust gas and take in,  
 195 which means that excessive air is needed. Fig.1 shows that the power stroke occurs in  
 196 the left cylinder and the scavenging process occurs in the right cylinder. The prototype  
 197 specifications and the values of the input parameters are listed in Table 1. Some  
 198 parameter settings refer to related literature [34]. TDC and BDC are the abbreviation  
 199 for top dead center and bottom dead center.

200 **Table 1**

201 The geometric parameters of FPEG.

Parameters	Value (Unit)
------------	--------------

Bore	52.5 (mm)
Maximum stroke	54.0 (mm)
Maximum effective intake flow area	1000 (mm <sup>2</sup> )
Maximum effective exhaust flow area	500 (mm <sup>2</sup> )
Intake port opening angle	108 (CA°,ATDC)
Intake port closing angle	108 (CA°,BTDC)
Exhaust port opening angle	80 (CA°,ATDC)
Exhaust port closing angle	80 (CA°,BTDC)

## 202 2.2 Description of scavenging problem

203 For conventional two-stroke combustion engine, the scavenging efficiency of the  
 204 cross-scavenging type is limited due to its relatively shorter gas changing time and  
 205 scavenging loss. Therefore, its thermal efficiency is considered to be worse than that of  
 206 the four-stroke combustion with independent intake/exhaust process. For a free-piston  
 207 engine, it can be seen as an unstable two-stroke internal combustion engine with  
 208 variable compression ratio that seems more difficult to control than a conventional  
 209 crankshaft two-stroke engine.

210 Since free-piston engines often operate under different conditions, it is obvious  
 211 that the engine stroke and corresponding compression ratio are variable. For traditional  
 212 cross-scavenging where the opening and closing angles of the valve is fixed, it cannot  
 213 always match with the working condition of the free-piston engine to achieve better  
 214 scavenging performance. Therefore, free piston engines cannot burn well organized air-  
 215 fuel mixture. If the air-fuel mixture falls outside the normal ignition range, it may result  
 216 in inadequate combustion or even a misfire. In addition, due to the elimination of  
 217 mechanical systems, the cyclic change of free-piston engine can make their scavenging  
 218 performance worse.

219 In order to develop free-piston engine, a more efficient system was designed to ensure  
 220 higher scavenging efficiency and to accommodate erratic operation. Variable-  
 221 scavenging-timing technology is considered to be a strategy for improving performance.  
 222 It is advised that the intake/exhaust valves are installed in the intake/exhaust ports,  
 223 which can achieve the stepless adjustment of the intake/exhaust flow area. In this way,  
 224 the degree of valve opening can be controlled to change the effective area of  
 225 intake/exhaust ports. The effective area of intake/exhaust ports is depended on the  
 226 operation rather than the piston motion. Similarly, the opening and closing of  
 227 intake/exhaust can be decided by the operation on the intake/exhaust valve. And their  
 228 time about the opening and closing also can be controlled to change the scavenging  
 229 progress.

230 However, due to the lack of research on the actual scavenging process of FPEG,  
 231 researchers may set too high scavenging parameters in the simulation, and it is often  
 232 difficult to achieve the expected value in the experiment. In order to verify the  
 233 improvement of FPEG performance by variable-scavenging-timing technology, the

234 numerical simulation and simulation are emphatically carried out in this paper.  
235 According to the characteristics of FPEG, three instabilities are considered in this  
236 study, and the detailed results will be given in the next chapter:  
237 a) The operation in different frequencies with fixed ignition time and stroke;  
238 b) Different compression ratios with fixed stroke and frequency;  
239 c) The cyclic variation at the same frequency and compression ratio.

## 240 **3 Numerical modelling and simulation method**

### 241 *3.1 Numerical modelling*

#### 242 *3.1.1 The FPEG dynamic equations*

243 During the operation of the FPEG system, the forces acting on the pistons with the  
244 mover are generally composed of four parts, *i.e.* the in-cylinder gas forces from each  
245 cylinder, the electromagnetic force of the linear electric machine, the frictional force  
246 from the mechanical parts, and the inertial force of the moving parts. According to  
247 Newton's second law, the dynamic equations of the piston can be expressed as:

$$248 \quad m \frac{d^2x}{dt^2} = F_l - F_r - F_f - F_g \quad (1)$$

249 where  $m$  (kg) is the mass of the left piston,  $x$  (m) is the displacement of the piston,  $F_l$   
250 (N) is the in-cylinder gas force from the left cylinder,  $F_r$  (N) is the in-cylinder gas  
251 force from the right cylinder,  $F_f$  (N) is the frictional force the assembly of the piston  
252 needs to be overcome during the operation,  $F_g$  (N) is the resistance force from the  
253 linear electric motor when it acts as a generator.

254 The frictional force implemented on the piston and the connecting rod is usually  
255 dominated by viscosity friction of lubricating oil, which can be described as:

$$256 \quad F_f = C_f \frac{dx}{dt} \quad (2)$$

257 where  $C_f$  (N/m·s<sup>-1</sup>) denotes the viscosity friction coefficient.

258 In the process of stable operation, the linear electric machine is used as a generator  
259 to provide resistance force. Based on the electromagnetic theories, the resistance  
260 force  $F_g$  (N) can be expressed as:

$$261 \quad F_g = K_v \cdot v \quad (3)$$

262 where  $K_v$  (N/(m·s<sup>-1</sup>)) represents the coefficient of electromagnetic resistance,  $v$  (m/s)  
263 is the velocity of the piston.

### 264 3.1.2 Definition of scavenging performance

265 The amount of fresh air or air/fuel mixture entering the cylinder in each cycle is  
266 an important indicator to evaluate the quality of the engine's gas exchange process, and  
267 there are three parameters for evaluation, *i.e.* scavenging efficiency, delivery ratio the  
268 mass of intake gas flow and trapping efficiency.

269 The scavenging efficiency reveals the quality of scavenging, which is defined as:

$$270 \quad \eta_s = \frac{m_o}{m_o + m_r} \quad (4)$$

271 where  $\eta_s$  is the scavenging efficiency, which is usually between 0.7 and 0.9.  $m_o$  (kg)  
272 is the mass of fresh air trapped in the cylinder and  $m_r$  (kg) is the mass of the exhaust  
273 gas that is trapped in the cylinder.

274 The delivery ratio is applied to describe the ability of absorbing fresh air, and can  
275 be given as:

$$276 \quad \eta_{dr} = \frac{m_t}{m_{sv}} \quad (5)$$

277 where  $\eta_{dr}$  is the delivery ratio, which is normally in the range of 1.0 to 1.5 without  
278 the crankcase (when there is a crankcase, it is then supposed to be from 0.5 to 0.9).  $m_t$   
279 (kg) is the mass of the intake air.  $m_{sv}$  (kg) is the mass required to fill the swept volume.

280 The intake air mass is expressed by the equation. Ignoring the effect of temperature  
281 difference, the mass of intake air can be expressed as:

$$282 \quad \dot{m} = \frac{60\rho v_m}{n} \int_{\phi_2}^{\phi_1} A_f \quad (6)$$

283 where  $\dot{m}$  (kg/s) is the instantaneous air flow.  $\rho$  (kg/m<sup>3</sup>) is gas density at the inlet  
284 manifold.  $v_m$  (m/s) is the total average flow velocity at the port.  $n$  (rpm) is the engine  
285 speed of FPEG.  $\phi$  (CA°) is the angle of the intake-air port and  $A_f$  (m<sup>2</sup>) is the  
286 instantaneous cross section area of air flow when the intake port is open.

287

288 The trapping efficiency is defined by the equation:

$$289 \quad \eta_{te} = \frac{m_o}{m_t} \quad (7)$$

290 where  $\eta_{te}$  is the trapping efficiency, which is usually less than 0.9.

### 291 3.1.3 Thermodynamic model

292 To estimate the completion of FPEG combustion, a single-zone Wiebe function is  
293 employed for depicting the proportion of burned fuel and is expressed as:

$$294 \quad x_b = 1 - \exp \left[ -a \left( \frac{t-t_0}{\Delta t} \right)^{m+1} \right] \quad (8)$$

295 where  $x_b$  is the mass fraction burned,  $t_0$  (CA°) is the beginning of the

296 combustion,  $\Delta t$  (CA°) is the duration of the combustion which stems from the  
 297 magnanimous experimental data and  $m$  is the parameter to fit the actual mass fraction  
 298 burned curve, which is usually taken as 2.  $a$  is also a constant that can be changed to  
 299 meet the computational needs, and is typically defined as 5 in the two-stroke  
 300 combustion.

301 With regard to heat transfer coefficient  $h_c$ , Woschni's correlation is used to  
 302 calculate the heat transfer loss, which is written as

$$303 \quad h_c = CB^{\eta-1} p_c^\eta \omega^\eta T_c^{0.75-1.62\eta} \quad (9)$$

304 where the bore length  $B$  (m) determined for the characteristic length,  $p_c$  (Pa)  
 305 and  $T_c$  (K) are the cylinder pressure and temperature respectively,  $C$  and  $\eta$  are empirical  
 306 parameters, and the gas velocity  $\omega$  (m/s) is used for a two-stroke engine without swirl.

### 307 *3.1.4 Main evaluation indexes of the performance*

308 For the overall engine performance of the FPEG, it occurs in brake power and its  
 309 indicated efficiency. They are expressed as

$$310 \quad P_b = \frac{\bar{p}_b V_s \eta_i}{30} \quad (10)$$

$$311 \quad \eta_i = \frac{3.6 \times 10^3}{H_u b_i} \quad (11)$$

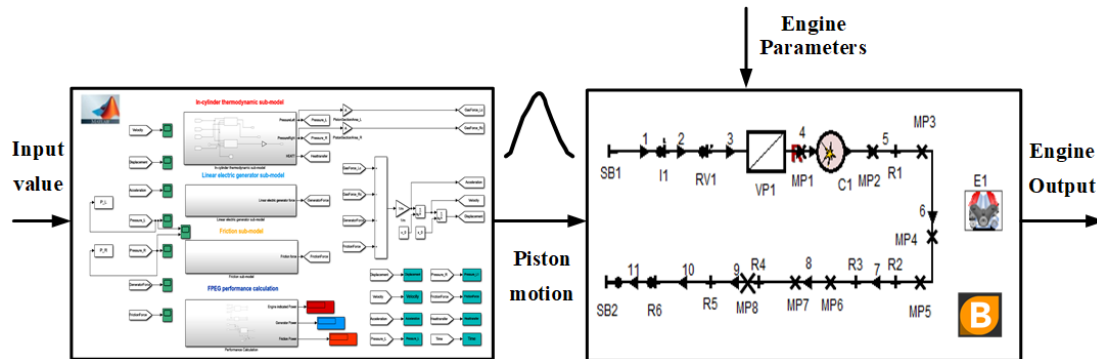
$$312 \quad V_s = LA \quad (12)$$

313 where  $\eta_i$  is the indicated efficiency,  $b_i$  (g/(kW·h)) is the fuel consumption per hour  
 314 and  $H_u$  (MJ/Kg) is the low heating value of the fuel.  $P_b$  (Kw) is the brake power of the  
 315 free-piston engine,  $L$  (m) is the piston stroke,  $A$  (m<sup>2</sup>) is the area of the piston,  $V_s$  (m<sup>3</sup>)  
 316 is the volume at which the engine sweeps and  $\bar{p}_b$  (MPa) is the mean effective pressure  
 317 of the brake.

### 318 *3.2 Simulation method*

319 Matlab/Simulink and AVL Boost are used for coupling simulation of the system  
 320 model. As mentioned earlier, the force acting on the piston can be divided into three  
 321 main types: the gas force generated by the left and right cylinders, the electromagnetic  
 322 force generated by the linear generator, and the friction force acting in the opposite  
 323 direction of the piston motion. According to the dynamics formula in Section 3.1.1, the  
 324 piston displacement profile was obtained through the Matlab/Simulink model. Fig.3  
 325 represents four sub-models in the simulation model. The in-cylinder gas force sub-  
 326 model takes compression/expansion, gas ignition, scavenging and heat transfer into  
 327 account. The friction sub-model is generally used to calculate the friction force arising  
 328 from the piston rings and the cylinder wall during the operation. Friction is the  
 329 resistance opposite to the direction of the piston velocity. The force sub-model of linear  
 330 motor mainly describes the force that FPEG drive component receives due to

331 electromagnetic shock during operation. The results of Matlab/Simulink model are  
 332 imported into AVL BOOST to simulate the characteristics of FPEG. Detailed model  
 333 description and validation results of the Matlab/Simulink model can be found the  
 334 authors' previous publications [35].



335  
 336 **Fig. 3** Matlab & AVL Boost combined simulation illustration

337 The traditional two-stroke structure is used for modeling, and the pumping loss  
 338 and most of the combustion loss are not considered when simplified. In the AVL  
 339 BOOST model, some initialization settings are required such as inlet and outlet  
 340 environment, initial temperature in cylinder and some thermal parameters, and the key  
 341 features are indicated in Table 2. Some of the combustion-related settings refer to some  
 342 literature and previous experiments [36].

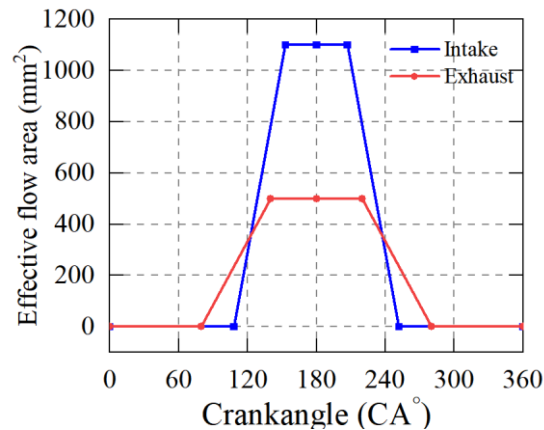
343 **Table 1**

344 The primary initial parameters

Parameters	Value (Unit)
System operating frequency	30 (Hz)
Inlet temperature	293 (K)
Inlet pressure	1.181 (bar)
Outlet temperature	500 (K)
Outlet pressure	0.981 (bar)
Air-to-fuel ratio	12.5
Geometrical crankcase compression ratio	1.2
Initial combustion duration	40 (CA°)
Initial start of combustion	15 (CA°, BTDC)

345 Considering that the cylinder head is scavenged by orifice, it is suggested to  
 346 introduce the curve of effective flow area in the cylinder modular. Fig.4 is the section  
 347 of the effective flow area measured from the cylinder used in the design prototype. Due  
 348 to the limitation of the actual size of the intake and exhaust ports, the effective flow  
 349 area has a certain range. Different effective flow area distributions are used at the intake  
 350 and exhaust ports to facilitate the scavenging process. Under flexible operating  
 351 conditions, these scavenging angles could be changed by piston movement. For  
 352 example, it is assumed that the opening Angle of the intake timing can be adjusted to  
 353 ensure that there is sufficient fresh air to remove residual heat in the cylinder. The  
 354 effective flow area profile of the piston motion based on the geometry of the prototype

355 combined with the design will be implemented in the AVL BOOST model



356

357

**Fig. 4** Effective flow area illustration

358

359

360

361

362

363

364

365

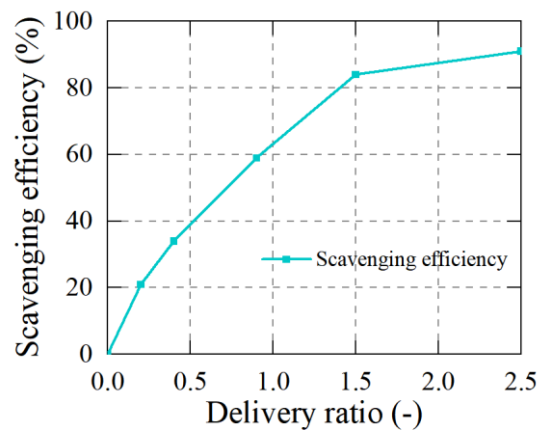
366

367

368

369

In academic articles, two simple models for scavenging, namely perfect displacement model and complete mixing model, are introduced as the boundary of scavenging performance. The former model assumes that the intake gas and the combustion gas do not mix, while the latter assumes that the intake gas and the combustion gas mix completely and instantaneously. The former model implies the upper bound of the scavenging efficiency, while the latter one implies the lower bound. Most of the scavenging efficiency curves designed by users are obtained by these models, which are in line with the actual data and expected indicators. Although the shapes of different simulation curves are different, scavenging efficiency generally tends to be positively correlated with delivery ratio. In AVL Boost's simulation, it is used by the user to define the purge model. In this article, the curve is plotted in Fig.5, which is based on some reference[37].



370

371

**Fig. 5** User-defined scavenging efficiency

372

373

374

During the operating of the FPEG, the engine compression ratio and stroke could be flexibly changed according to different working conditions while the engine design parameters remain unchanged throughout the simulation. Five simulation cases of

375 different working conditions are selected to further discuss the influence of different  
 376 working conditions on the scavenging characteristics and engine performance of FPEG,  
 377 as shown in Table 3.  $\epsilon$  represents the compression ratio and Var refers to the cyclic  
 378 variation near the TDC. The different combustion durations at the different compression  
 379 ratios are 45 CA°( $\epsilon=7$ ), 44 CA°( $\epsilon=8$ ), 43 CA°( $\epsilon=9$ ), 42 CA°( $\epsilon=10$ ) and 41 CA°( $\epsilon=11$ ).  
 380 The starts of combustion are before bottom dead center 15 CA°( $\epsilon=7$ ), 14 CA°( $\epsilon=8$ ), 13  
 381 CA°( $\epsilon=9$ ), 12 CA°( $\epsilon=10$ ) and 11 CA°( $\epsilon=11$ ). As for the other cases, they are maintain  
 382 the original setup.

383 **Table 3**

384 Simulation cases with different working conditions

Parameters (Unit)	Case 1	Case 2	Case 3	Case 4	Case 5
$\epsilon$ (-) (Var=0, frequency=30 Hz)	7	8	9	10	11
	Case 6	Case 7	Case 8	Case 9	Case 10
Var (mm) ( $\epsilon=7$ , frequency=30 Hz)	-2	-1	0	1	2
	Case 11	Case 12	Case 13	Case 14	Case 15
Frequency (Hz) ( $\epsilon=7$ , Var=0)	28	29	30	31	32

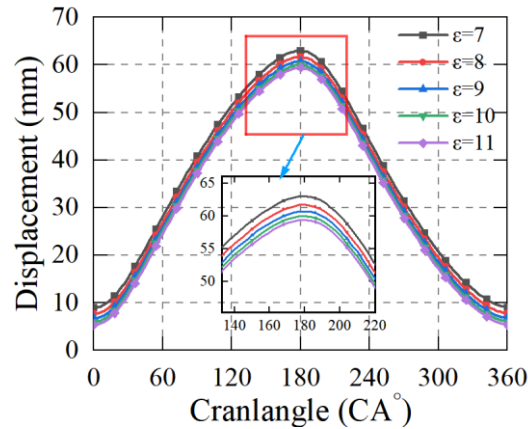
385 In addition, cyclic variations should be taken into account. The variable-  
 386 scavenging-timing technology also focuses on the partial optimization of scavenging.  
 387 In order to highlight the advantages of variable-scavenging-timing technology, the  
 388 displacement generated by Matlab is applied to the operation of the AVL BOOST model,  
 389 which has different changes in each cycle. According to the displacements, the curves  
 390 of effect flow area fluctuate within an appropriate range. Its function is to keep the  
 391 FPEG proper air intake and scavenging smoothly.

## 392 **4 Results and discussion**

### 393 *4.1 Influences with different compression ratios*

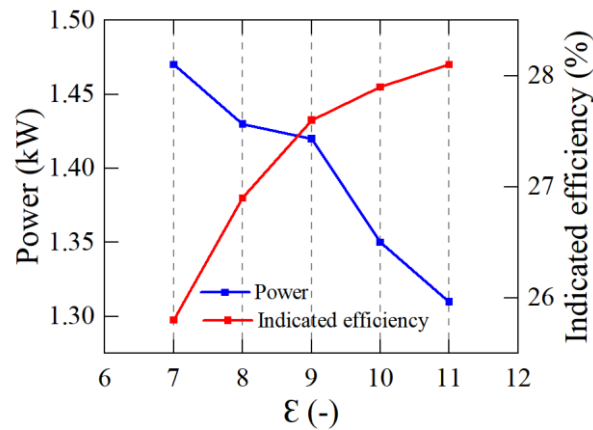
394 The prototype usually works at a compression ratio of 10 and a stroke of 54 mm.  
 395 However, due to the lack of stability, different compression ratios are produced in  
 396 operation. As shown in Fig.6, displacement also shows diversity. Each compression  
 397 ratio corresponds to its own stroke, TDC and BDC. Under the condition of constant

398 stroke, the increase of compression ratio is closely related to the contraction of piston  
 399 displacement and the backward shift of TDC and BDC. Different compression ratio  
 400 would destroy the dynamic balance of piston motion, so that the piston deviates from  
 401 the ideal operating range. At this time, the existing working conditions often conflict  
 402 with the piston movement displacement. Scavenging, combustion and other processes  
 403 are more or less affected. Obviously, the performance of FPEG is far from satisfactory.



404  
 405

**Fig. 6** Displacement with different compression ratios



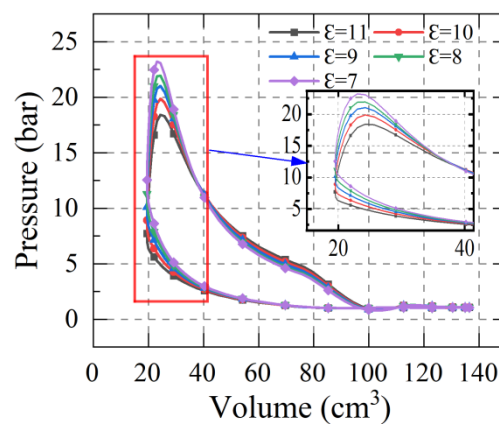
406  
 407

**Fig. 7** Performance with different compression ratios

408 The amplitude of the power and indicated efficiency are shown in Fig.7. The  
 409 results show that the highest indicating efficiency is about 28.1 % and the lowest  
 410 indicating efficiency is about 25.8 %. The maximum power and minimum power of  
 411 cross scavenging are 1.47 kW and 1.31 kW. In these cases, it can be learned that the  
 412 indicated efficiency increased with the increase of compression ratio. In other words,  
 413 the amplification of the indicated efficiency does not seem to have reached its limits,  
 414 implying that there is still room for optimization. On the contrary, power has a tendency  
 415 not to rise at higher levels. It is pointed out that this piston motion may be suitable for  
 416 medium compression ratio.

417 The indicated efficiency is positively correlated with the compression ratio from

418 many angles, but the power does not always behave well on this PFEF. In fact, this  
 419 piston motion of FPEG is different from traditional two-stroke combustion and may not  
 420 match past experience and is reflected in practice. Irregular piston movement  
 421 displacement, which means the piston motion of FPEG is unlike traditional two-stroke  
 422 internal combustion engine and usually asymmetry is more sensitive to slight changes  
 423 representing the instability in compression ratio, movement frequency and the variation  
 424 which could lead to the different performance and scavenging quality, which might lead  
 425 to abnormal phenomena presented as fluctuation in performance or the other evaluation  
 426 index. Therefore, different compression ratios directly affect pressure transformation.  
 427 As can be seen from Fig.8, the scavenging time is too long and the inlet and exhaust  
 428 angles overlap greatly, which might lead to the difficulty in effective operation of some  
 429 strokes because the pressure at this time is close to the intake pressure. The higher the  
 430 compression ratio, the more serious the situation. As can be seen from Fig.8, the  
 431 equivalent is relatively low, and the maximum pressure is inconsistent with the demand  
 432 at high power, which also explains the reason why the power is not high enough in the  
 433 design and simulation.



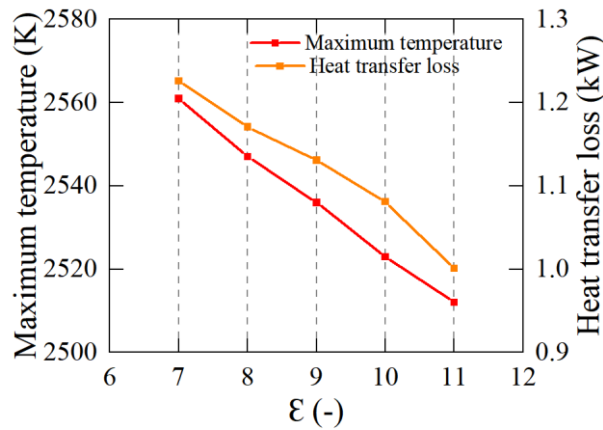
434

**Fig. 8** P-V with different compression ratios

435

436 In addition, continuous improvement in indication efficiency is noted. For one  
 437 thing, in this case, the speed is almost constant, and the settings are the same except for  
 438 the compression ratio. Therefore, according to the above discussion, fuel loss, friction  
 439 loss and other losses should not differ much. For another thing, the heat transfer loss  
 440 accounts for a large proportion of the total energy consumption. There is an obvious  
 441 change in heat transfer loss in Fig.9. As the compression ratio increases, the heat  
 442 transfer loss decreases. Because in this case, the higher the compression ratio is, the  
 443 lower the maximum temperature is. Temperature difference is related to heat transfer  
 444 loss. Although power might be limited by high compression ratios for various reasons,  
 445 the percentage of power in the effective power increases as losses decrease. From this  
 446 perspective, it is understandable why the high compression ratio in this paper leads to  
 447 high indicating efficiency. Therefore, as the compression ratio increases, the FPEG has  
 448 higher indicating efficiency, but more energy is consumed in the other part of the

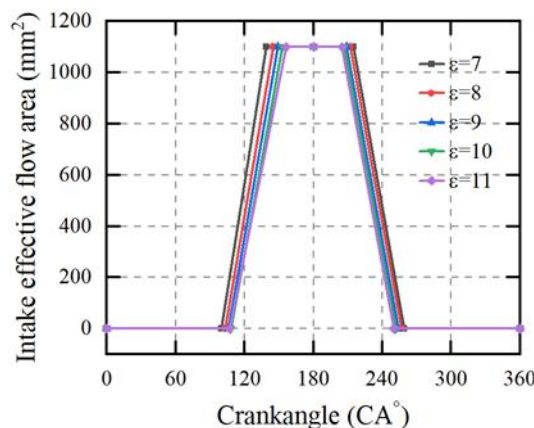
449 braking power output, indicating that the model is suitable for medium compression  
450 ratio when piston movement and other conditions are similar to the simulation settings.



451

452 **Fig. 9** Maximum temperature and heat transfer loss with different compression ratios

453 Compression ratio not only affects mechanical properties, but also changes  
454 scavenging rate. The scavenging process is managed by piston movement due to the  
455 use of scavenging with vents. Fig.10 and Fig.11 shows the different effective flow area  
456 of intake/exhaust for different compression ratios. With the influence of compression  
457 ratio on piston movement and displacement, scavenging capacity also change. As can  
458 be seen from Fig.12, scavenging efficiency between different compression ratios tend  
459 to have a small gap. The highest scavenging efficiency is 86.7 % and the lowest is  
460 85.1 %. The delivery curve fluctuates gently. It can climb as high as 1.671 or as low as  
461 1.66. The scavenging efficiency curve is wavy, indicating the existence of compression  
462 ratio, which makes the FPEG work inefficiently. As a result of the use of user-defined  
463 models, as mentioned in Section 3.1.2, the delivery ratio largely determines the  
464 scavenging efficiency. The delivery ratio has a great influence on scavenging efficiency,  
465 and the similar delivery ratio leads to the similar scavenging efficiency.



466

467

**Fig. 10** Intake effective flow area with different compression ratios

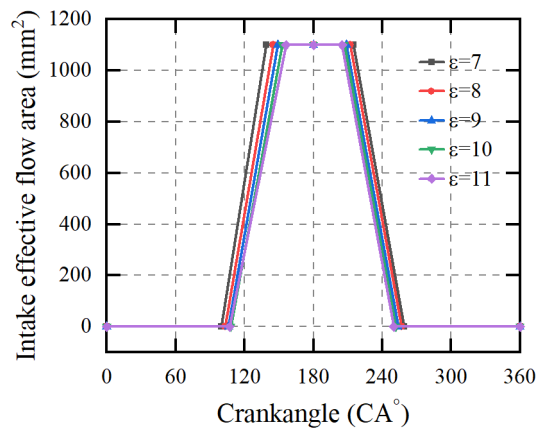


Fig. 11 Exhaust effective flow area with different compression ratios

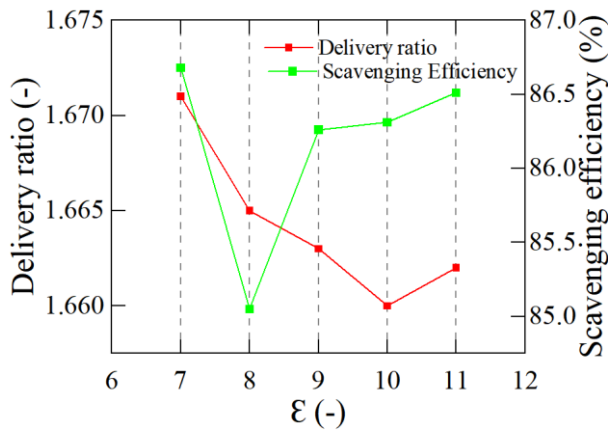
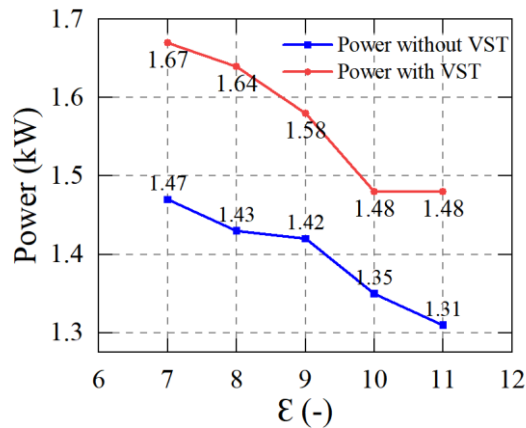


Fig. 12 Delivery ratio and scavenging ratio with different compression ratios

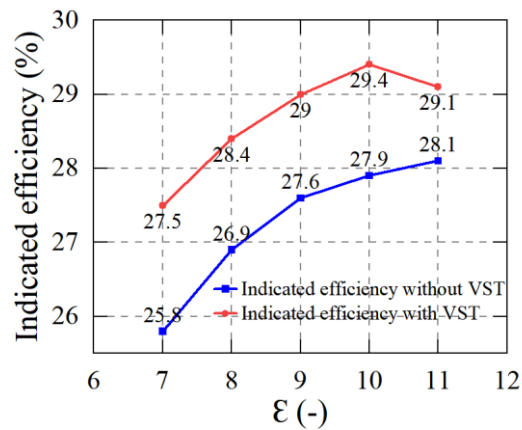
Due to the constant opening and closing time of traditional cross-flow scavenging, the FPEG cannot show its advantages over traditional two-stroke engine in this scavenging mode. FPEG can benefit from variable-scavenging-timing technology when ignition time, fuel injection volume, and other setting conditions that affect performance remain constant. According to the results of previous studies, it is suggested that the overlap of scavenging angle should be reduced to reduce unnecessary scavenging loss. The results indicate that the opening angle of intake is adjusted from 108 CA° to 120 CA° and the closing angle of intake is changed from 252 CA° to 240 CA°. At these compression ratios at which FPEG works, the machine integrated with variable-scavenging-timing technology tends to perform better. In terms of power, the FPEG with this technology is obviously more ideal. After several iterative calculations, the power in Fig.14 remains above 1.45 kW. As can be seen from Fig.13, the FPEG using variable-scavenging-timing technology (VST) works at an indicated efficiency of no less than 27 %, which is more efficient and more stable than the cross-scavenging FPEG. There are obvious differences between the two descriptions for the delivery ratio

488 generated by different scavenging modes.



489  
490

Fig. 13 Comparison of the power



491  
492

Fig. 14 Comparison of indicated efficiency

493 There are many reasons for the above phenomenon, and the main consideration is  
494 the possibility related to scavenging. The variable-scavenging-timing technology  
495 enables scavenging process to adapt to different compression ratio, reduces unnecessary  
496 gas loss, and makes scavenging more effective. Due to the control of fuel injection ratio,  
497 FPEG has a similar combustion environment, resulting in the same trend of power  
498 variation under such conditions. In other words, the variable-scavenging-timing  
499 technology may be beneficial to improving electricity and maintaining its regular  
500 pattern, since there is sufficient gas mixture to burn. This functionality is beyond the  
501 scope of cross scavenging.

502 In terms of indicated efficiency, the FPEG using variable-scavenging-timing  
503 technology is superior to that using cross scavenging. On the one hand, it is clear that  
504 variable-scavenging-timing technology offers more appropriate magnitude of fresh air  
505 for the mixture of air and fuel. The correct air-fuel ratio means that the combustion has  
506 reached one of the best initial conditions, requiring no additional air or fuel to produce  
507 the same amount of power. On the other hand, this new technology also has better

508 performance to capture gas in cylinders. As it can be seen from Fig.15, this new  
 509 technology has enhanced absorbability of fresh air at the specified compression ratio.  
 510 The new trapping efficiency has been improved 13 % or so higher on average. Trapping  
 511 efficiency in FPEG operations can make a remarkable difference in performance. It is  
 512 reasonable to speculate that the variable-scavenging-timing technology is beneficial to  
 513 reduce the possibility of over-scavenging and air leakage, and to improve the economy  
 514 of the machine.

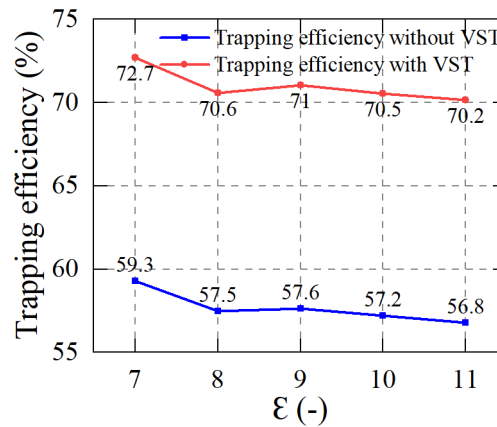
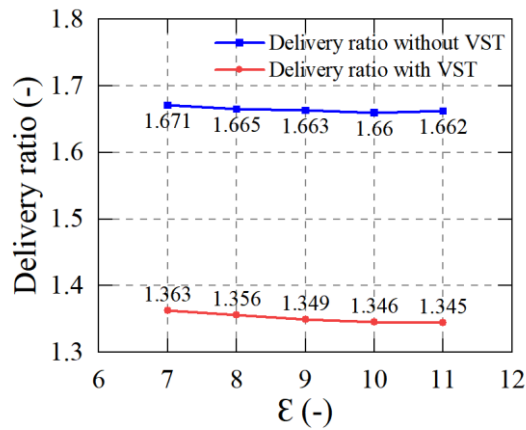


Fig. 15 Comparison of trapping efficiency

515  
 516  
 517 For scavenging efficiency under different compression ratios, it can be seen that  
 518 the synergistic effect of variable-scavenging-timing technology and piston motion  
 519 significantly determines scavenging process and volumetric efficiency, meaning that  
 520 the vast majority of fresh air is used to clean up residues and air-fuel mixtures. Too long  
 521 scavenging process would take in excessive cold air, which might cool mixed gas, and  
 522 too short scavenging time would result in insufficient air to burn. Although the three-  
 523 dimensional structure of scavenging parts is not considered, scavenging loss may be  
 524 slightly reduced in the zero-dimensional simulation due to the coordinated operation  
 525 mode of scavenging parts. In addition, the custom scavenging model defined in Section  
 526 3.3.2 has the greatest impact on the calculation of scavenging efficiency. It can be  
 527 predicted that the variable-scavenging-timing helps to maintain a stable delivery ratio.  
 528 It could be inferred that the delivery ratio without variable-scavenging-timing  
 529 technology is about 1.66, for which the corresponding scavenging efficiency is  
 530 remained about 0.86 according to the curve of relationship about scavenging efficiency  
 531 and delivery ratio. In Fig.16, delivery ratio decreases by an average of about 0.3. Based  
 532 on previous research, with constant power, a lower delivery ratio might help reduce the  
 533 amount of fresh air available for combustion, thus reducing fuel costs. Meanwhile, the  
 534 volumetric efficiency gets improved indirectly. They promote more mixture gas to  
 535 staying in the cylinder. Finally, it also gives a positive feedback in performance.



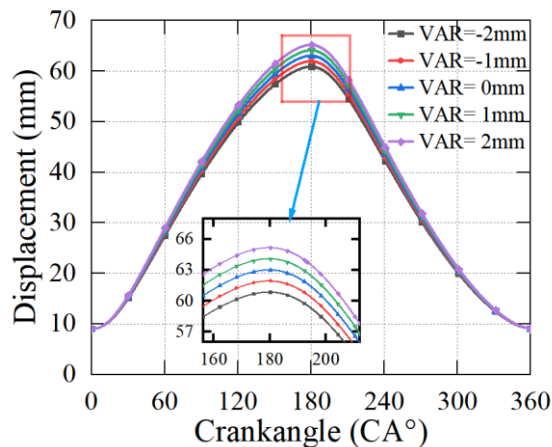
536

537

Fig. 16 Comparison of the delivery ratio

#### 538 4.2 Discussion on cyclic variations

539 Given the instability of piston motion, there are many other forms besides different  
 540 compression ratios. For example, the effect of cyclic change on purification efficiency  
 541 and other evaluation criteria is worth discussing. In fact, cyclic variation can take many  
 542 forms, such as early or late arrival at the TDC, sudden acceleration or deceleration in  
 543 motion, etc. Fig.17 shows several classical displacements with different cyclic  
 544 variations, and the compression ratio is approximately regarded as 7, and the simulation  
 545 ignores the fluctuation of working frequency.



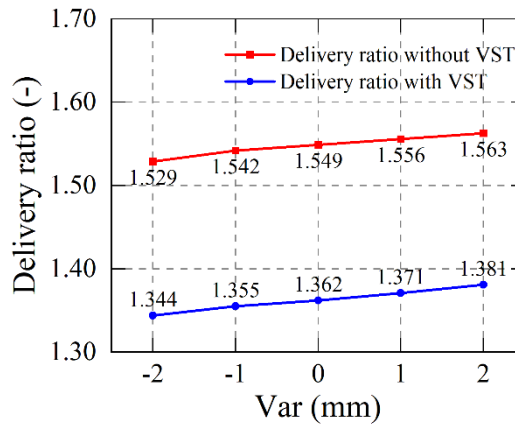
546

547

Fig. 17 Displacement with different variations

548 When the traditional cross-scavenging method is used, the cyclic variation of two-  
 549 stroke combustion will affect the scavenging process. It can be seen from Fig.18 that  
 550 the cyclic variation in the figure leads to the irregular drift of the transport ratio, and  
 551 there is a gap between the normal curve and other curves in the figure without the  
 552 variable-scavenging-timing technology. The results show that the lowest fuel supply  
 553 ratio is 1.529, the highest is 1.563, and its fluctuation corresponds to the curve of piston

554 displacement with cyclic variation. In addition, the cyclic variation causes the piston to  
 555 do extra work, which results in a small additional energy consumption in terms of  
 556 frictional power or heat transfer loss (as mentioned in Section 3.2, other parts of the  
 557 energy loss may be ignored). The friction power consumption is larger when the three-  
 558 dimensional structure is considered.

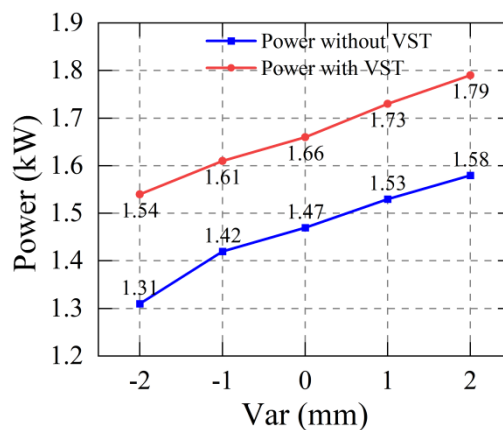


559

**Fig. 18** Comparison of the delivery ratio

560

561 The impact of scavenging, which is rooted in the cyclic variation, ultimately  
 562 affects performance. In the Fig.19, the attenuation of FPPEG power with a change of less  
 563 than 0 is represented. According to the fixed setting, note that the initiation of  
 564 combustion occurs simultaneously with insertion rather than with the corresponding  
 565 cyclic variation, which means that the mixture of air and fuel is improperly affected by  
 566 the cyclic change or the ignition combustion time is not ideal. In fact, cyclic variation  
 567 requires many parameters to accommodate multivariate displacement in order to  
 568 transform a good thermodynamic environment. In addition, cyclic variation may also  
 569 produce some force asymmetries, leading to dysfunction.



570

571

**Fig. 19** Comparison of the power

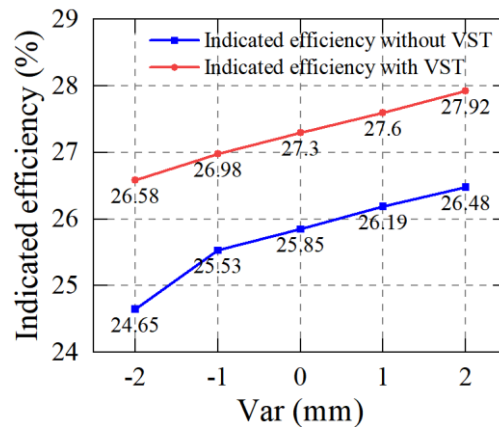


Fig. 20 Comparison of the power

572

573

574 This bad performance is reversed when variable sweep speed regulation  
 575 technology is adopted. In contrast to the cross-scavenging method, Fig.18 shows that  
 576 the variable-scavenging-timing technology helps reduce fresh air consumption with the  
 577 cyclic variation. The Fig.19 and Fig.20 show the variable-scavenging-timing  
 578 technology improves the performance. The results show that the power and indicating  
 579 efficiency are improved to some extent. Compared with cross scavenging, the delivery  
 580 ratio is 1.381, much lower than before. Power and indicating efficiency are kept in a  
 581 better state than before. Although the variable-scavenging-timing technology cannot  
 582 completely suppress the effect of cyclic variation, when it is greater than 0, it seems  
 583 that the variable-scavenging-timing technology could hardly make its performance  
 584 equal to the variation of 0, which indicates that cyclic variation is important to deal with.  
 585 Otherwise, the more variations occur, the worse performance would be.

### 586 4.3 Consequences about variable frequency

587 Despite cyclic variation and the change about frequency occur simultaneously in  
 588 practice, for simultaneous analysis, it is divided into two parts. Section 4.2 discusses  
 589 the displacement of cyclic variation. Here, it is mainly about the difference of frequency  
 590 without considering the change of displacement frequency. The range of frequency  
 591 variation lists in Table.3 is small. Otherwise, the operation environment is not stable or  
 592 the apparatus is not running well.

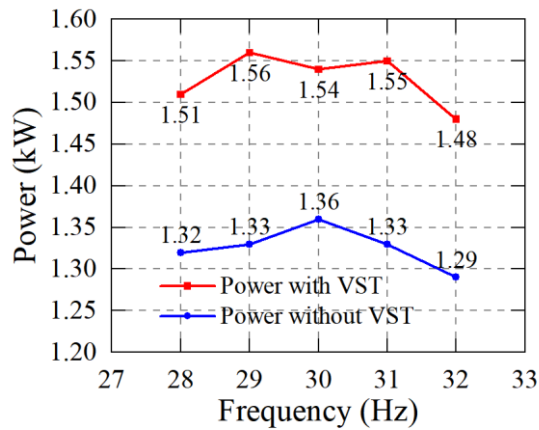


**Fig. 21** Comparison of power

Predictably, a change in frequency makes the difference. According to Fig.21, the maximum power is 1.36 kW and the minimum power is 1.29 kW. Meanwhile, the variable frequency has little influence on the power, which results from the fixed working-volume. There seems to be a spike in this trend, which means that 30 Hz may be the best operating frequency in this range. As can be seen from Fig.22, the increase in frequency promotes the indicated efficiency, while the increase in frequency promotes the mixing of fresh air and fuel. The highest indicating efficiency is 25.76 %, the lowest is 24.62 %, so there is a lot of room for improvement. As for the delivery ratio, it is clear that the frequency is inversely correlated with the transport ratio. When the frequency reaches the lowest value, the delivery ratio is 1.62. Conversely, the highest frequency corresponds to the lowest delivery ratio of 1.43, because the increasing frequency is equivalent to the decreasing scavenging time. In the case that the scavenging environment remains unchanged, the intake mass usually declines, while the retention mass remains at a stable state. Therefore, according to the theory in Section 3.1.2, the delivery ratio becomes smaller.

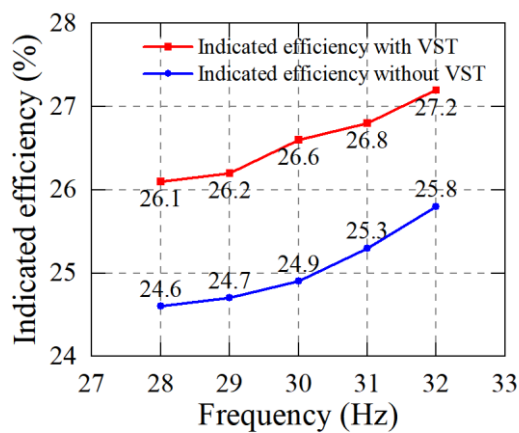


**Fig. 22** Comparison of indicated efficiency

593

594

595

596

597

598

599

600

601

602

603

604

605

606

607

608

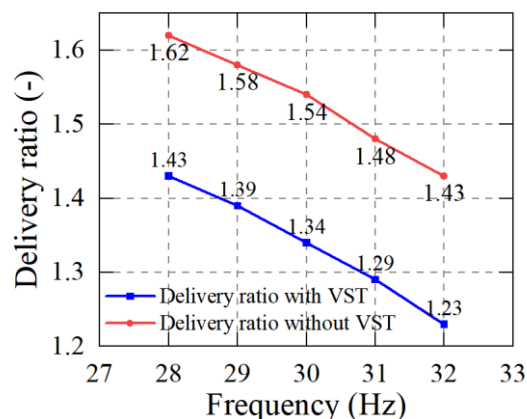
609

610

611

612

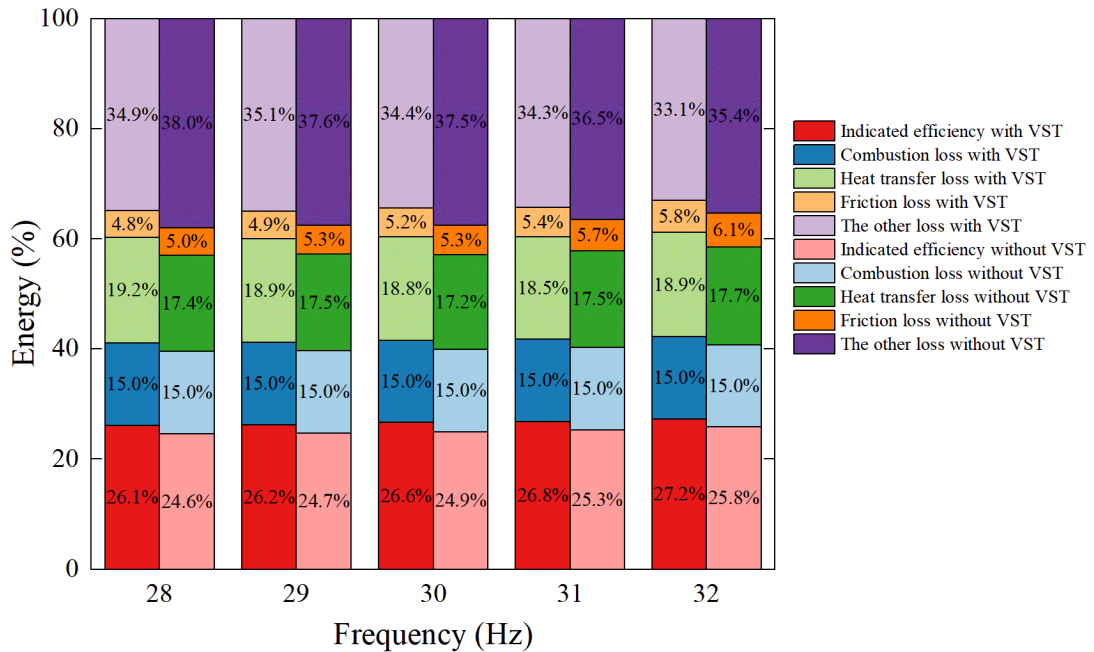
613 Through the optimization with the variable-scavenging-timing technology, it can  
 614 be seen from the Fig.21 and Fig.22 that part of the performance deteriorated by  
 615 frequency conversion is improved. With the application of the variable-scavenging-  
 616 timing technology, the performance of the FPEG in this interval is improved by a notch.  
 617 The new maximum power is 1.56 kW and the new minimum power is 1.48 kW. The  
 618 new highest indicated efficiency is 27.2 % and the lowest is 26.1 %. Although the value  
 619 is increased, the curve has a similar trend. From the preliminary analysis, the variable-  
 620 scavenging-timing technology still keeps the FPEG staying in the normal working  
 621 condition. That is why the curves of the performance have a similar shape. Similar to  
 622 the performance results, the delivery ratio with VST is improved, and the shape of the  
 623 delivery ratio curve is not different from that without VST. In the Fig.23, the new  
 624 maximum and minimum delivery ratio is 1.43 and 1.23. In the absence of VST, they  
 625 are all less than the minimum output ratio. It can be inferred that this technology can  
 626 effectively reduce the quality of incoming fresh air or escaping gas. Most of the gas is  
 627 burned, rather than exhausting the cylinder, and most of the intake forms a mixture of  
 628 gases, rather than being scavenged to the outside. Finally, within the same scavenging  
 629 efficiency range, the scavenging efficiency is between 85 % and 87 %, because in this  
 630 simulation, the curve of scavenging efficiency is defined by the user. When the delivery  
 631 ratio is more than 1.5, the scavenging efficiency increases slowly macroscopically.



632  
 633 **Fig. 23** Comparison of delivery ratio

634 Since the change of the operating frequency would cause the change of the piston  
 635 speed, the friction loss would also change. Therefore, the energy balance of FPEG  
 636 should also be considered in this unstable situation. In the Fig.24, it is known that the  
 637 energy balance varies with the operating frequency. High operating frequency has a  
 638 better indication of thermal efficiency while heat transfer loss is smaller. The  
 639 combustion loss is supposed to be assumed in the simulation, thus the combustion loss  
 640 is set to 15 % according to the many experiments and references. And “the other loss”  
 641 is the sum of all losses that are not listed separately, including pumping loss and exhaust  
 642 loss. It can be known from Fig.24 that additional friction loss would occur if some high-  
 643 frequency operating condition occurs during the movement of the piston. And there

644 would be more “the other loss” under low-frequency operating condition. After the  
 645 application of VST, it is obvious that the indicated efficiency and “the other loss” has  
 646 been optimized. It is clear that “the other loss” which has the proportion from 38 % to  
 647 35.4 % in the entire energy comes to a level of 33.1 % to 35.1 %. Although the heat  
 648 transfer loss has also increased by about 1 % to 2 %, the corresponding output power  
 649 has also increased according to Fig.21. It should be noted that the proportion of “the  
 650 other loss” in the entire energy loss is always large, and there is still a lot of space of  
 651 optimization for this problem in the future.



652  
 653 **Fig. 24** Energy balance at different frequencies

## 654 **5 Conclusion**

655 Improving scavenging efficiency and performance is a crucial challenge for  
 656 research on FPEG because it is not just about intake mass flow. It is often associated  
 657 with combustion, heat transfer, exhaust gas recycling and other important aspects of  
 658 performance. In this paper, the effects of two cross scavenging and variable-  
 659 scavenging-timing technology on FPEG are studied under different compression ratios,  
 660 cyclic variations and frequencies. By controlling variables, a series of cases are run in  
 661 AVL BOOST to obtain necessary results. And their effects on the scavenging efficiency  
 662 and other performances of FPEG are discussed. The results on the FPEG are  
 663 demonstrated by figures.

664 The results show that different compression ratio, cyclic variation and variable  
 665 frequency have some adverse effects on scavenging efficiency and other performance.  
 666 The change of compression ratios has a more negative impact on FPEG, especially on  
 667 power when the compression ratio is relatively high. The lower frequency and situation  
 668 that the piston cannot reach the design TDC both decrease performance and scavenging

669 quality of the FPEG. It is difficult to exactly predict or control the tendency of the piston  
670 motion in the actual experiment. The proportion of energy loss at different frequencies  
671 also shows that the technology has a lot of space for technological improvement and  
672 application prospects, especially in terms of some losses such as pumping loss and  
673 exhaust loss. Therefore, the variable-scavenging-timing technology is worth  
674 developing in the research of FPEG.

675 Once the variable-scavenging-timing technology is adopted, FPEG is very likely  
676 to have better performance under unsteady operation conditions. According to the  
677 simulation results, the delivery ratio of the FPEG applied with the variable-scavenging-  
678 timing technology is reduced by about 0.3 at different compression ratios, 0.18 at  
679 different cyclic variations and 0.2 at different frequencies on average. Especially under  
680 different compression ratios, the trapping efficiency of FPEG using VST has reached at  
681 least 70 %, which has been improved significantly compared to before. At the same  
682 time, in most cases, the scavenging efficiency is maintained at least 85% %. Under  
683 different compression ratios, the power increases by an average of 0.18 kW. While the  
684 power increases 0.2 kW on average under the other condition. The increase of indicated  
685 efficiency is in a varying range from 1 % to 2 % under unsteady conditions.

686 The variable-scavenging-timing technology can reduce the scavenging quality,  
687 which implies that the air-fuel ratio and combustion are in the appropriate stage. As a  
688 result, FPEG performance is unlikely to degrade. In addition, the variable-scavenging-  
689 timing technology pursues that the scavenging process gets along with the displacement  
690 of the piston. Trapping efficiency and the stability of scavenging are improved, which  
691 might be of great significance to the economy and reliability of FPEG. The variable-  
692 scavenging-timing technology can be driven in many ways, such as hydraulic drive,  
693 mechanical drive or electromagnetic drive, which implies many existing valve drive  
694 technologies may be integrated with it. Future work will focus on exploring the  
695 application scope of this technology and developing simple and effective actuators.

## 696 **Declaration of Competing Interest**

697 We declare that we have no financial and personal relationships with other people  
698 or organizations that can inappropriately influence our work, there is no professional or  
699 other personal interest of any nature or kind in any product, service and/or company  
700 that could be construed as influencing the position presented in, or the review of, the  
701 manuscript entitled.

## 702 **Acknowledgement**

703 This project is supported by the National Natural Science Foundation of China

704 (project number: 52005038, 51675043), and Beijing Institute of Technology Research  
705 Fund Program for Young Scholars. The authors would like to thank the sponsors.

## 706 Reference

- 707 1. Blair, G., *The basic design of two-stroke engines*. 1990: SAE.
- 708 2. Feng, H., et al., *Research on combustion process of a free piston diesel linear generator*. Applied  
709 Energy, 2016. **161**: p. 395-403.
- 710 3. Mikalsen, R. and A. Roskilly, *A computational study of free-piston diesel engine combustion*.  
711 Applied Energy, 2009. **86**(7-8): p. 1136-1143.
- 712 4. Zhao, Z., et al., *An experimental study of the cycle stability of hydraulic free-piston engines*.  
713 Applied Thermal Engineering, 2013. **54**(2): p. 365-371.
- 714 5. Guo, C., et al., *Advances in free-piston internal combustion engines: A comprehensive review*.  
715 Applied Thermal Engineering, 2021. **189**: p. 116679.
- 716 6. Raul, P., *Motor-compressor apparatus*. 1928, Google Patents.
- 717 7. Mikalsen, R. and A.P. Roskilly, *A review of free-piston engine history and applications*. Applied  
718 Thermal Engineering, 2007. **27**(14-15): p. 2339-2352.
- 719 8. Famouri, P., et al. *Design and testing of a novel linear alternator and engine system for remote*  
720 *electrical power generation*. in *IEEE Power Engineering Society. 1999 Winter Meeting (Cat.*  
721 *No. 99CH36233)*. 1999. IEEE.
- 722 9. Nandkumar, S., *Two-stroke linear engine*. 1998.
- 723 10. Houdyschell, D., *A diesel two-stroke linear engine,[electronic resource]*. 2000, West Virginia  
724 University.
- 725 11. Mikalsen, R. and A.P. Roskilly, *The control of a free-piston engine generator. Part 1:*  
726 *Fundamental analyses*. Applied Energy, 2010. **87**(4): p. 1273-1280.
- 727 12. Mikalsen, R. and A.P. Roskilly, *Performance simulation of a spark ignited free-piston engine*  
728 *generator*. Applied Thermal Engineering, 2008. **28**(14-15): p. 1726-1733.
- 729 13. Mikalsen, R. and A.P. Roskilly, *The design and simulation of a two-stroke free-piston*  
730 *compression ignition engine for electrical power generation*. Applied Thermal Engineering,  
731 2008. **28**(5-6): p. 589-600.
- 732 14. Mikalsen, R., E. Jones, and A.P. Roskilly, *Predictive piston motion control in a free-piston*  
733 *internal combustion engine*. Applied Energy, 2010. **87**(5): p. 1722-1728.
- 734 15. Jia, B., et al., *Analysis of the Scavenging Process of a Two-Stroke Free-Piston Engine Based on*  
735 *the Selection of Scavenging Ports or Valves*. Energies, 2018. **11**(2).
- 736 16. Jia, B., et al., *Piston motion control of a free-piston engine generator: A new approach using*  
737 *cascade control*. Applied Energy, 2016. **179**: p. 1166-1175.
- 738 17. Jia, B., et al., *Development and validation of a free-piston engine generator numerical model*.  
739 Energy Conversion and Management, 2015. **91**: p. 333-341.
- 740 18. Ngwaka, U., et al., *Parametric analysis of a semi-closed-loop linear joule engine generator*  
741 *using argon and oxy-hydrogen combustion*. Energy, 2020: p. 119357.
- 742 19. Fredriksson, J., et al., *Modeling the effect of injection schedule change on free piston engine*  
743 *operation*. 2006, SAE Technical Paper.

- 744 20. Bergman, M., J. Fredriksson, and V.I. Golovitchev, *CFD-based optimization of a diesel-fueled*  
745 *free piston engine prototype for conventional and HCCI combustion*. SAE International Journal  
746 of Engines, 2009. **1**(1): p. 1118-1143.
- 747 21. Goldsborough, S.S. and P. Van Blarigan, *Optimizing the scavenging system for a two-stroke*  
748 *cycle, free piston engine for high efficiency and low emissions: a computational approach*. SAE  
749 transactions, 2003: p. 1-20.
- 750 22. Sofianopoulos, A., et al., *Gas exchange processes of a small HCCI free piston engine - A*  
751 *computational study*. Applied Thermal Engineering, 2017. **127**: p. 1582-1597.
- 752 23. Lu, X., et al., *Analysis on Influences of Scavenging Ports Width to Scavenging Process Based*  
753 *on Opposed Piston Two Stroke Diesel Engine*, in *Innovative Solutions for Energy Transitions*, J.  
754 Yan, et al., Editors. 2019. p. 5838-5843.
- 755 24. Yuan, C., Y. Jing, and Y. He, *Coupled dynamic effect of combustion variation on gas exchange*  
756 *stability of a free piston linear engine*. Applied Thermal Engineering, 2020. **173**.
- 757 25. Yuan, C., et al., *Combustion characteristics analysis of a free-piston engine generator coupling*  
758 *with dynamic and scavenging*. Energy, 2016. **102**: p. 637-649.
- 759 26. Yuan, C., H. Ren, and J. Xu, *Comparison of the gas exchange of a loop scavenged free-piston*  
760 *engine alternator and the conventional engine*. Applied Thermal Engineering, 2017. **127**.
- 761 27. Yuan, C., Y. Jing, and Y. He, *Coupled dynamic effect of combustion variation on gas exchange*  
762 *stability of a free piston linear engine*. Applied Thermal Engineering, 2020. **173**: p. 115201.
- 763 28. Dong, X., et al., *Study on the Gas Consumption Characteristics of an Opposed-Piston Two-*  
764 *Stroke Engine*. Chinese Internal Combustion Engine Engineering, 2016. **37**(6): p. 216-221.
- 765 29. Mao, J., et al., *Multi-dimensional scavenging analysis of a free-piston linear alternator based*  
766 *on numerical simulation*. Applied Energy, 2011. **88**(4): p. 1140-1152.
- 767 30. GIBBES, G. and H. Guang, *Numerically Modeling the Dynamics of a Piston-Mounted Passive*  
768 *Inlet Poppet Valve*. 2007, SAE Technical Paper.
- 769 31. Wu, Y., et al., *Three-dimensional CFD (computational fluid dynamics) analysis of scavenging*  
770 *process in a two-stroke free-piston engine*. Energy, 2014. **68**.
- 771 32. Xu, Z. and S. Chang, *Prototype testing and analysis of a novel internal combustion linear*  
772 *generator integrated power system*. Applied Energy, 2010. **87**(4): p. 1342-1348.
- 773 33. Huihua, F., et al., *Investigation of the optimum operating condition of a dual piston type free*  
774 *piston engine generator during engine cold start-up process*. Applied Thermal Engineering,  
775 2021. **182**.
- 776 34. Jia, B., et al., *Investigation of the Starting Process of Free-piston Engine Generator by*  
777 *Mechanical Resonance*. Energy Procedia, 2014. **61**: p. 572-577.
- 778 35. Zz, A., et al., *Effect of the stroke-to-bore ratio on the performance of a dual-piston free piston*  
779 *engine generator*. Applied Thermal Engineering, 2020. **185**.
- 780 36. Belgiorno, G., et al., *Parametric Analysis of the Effect of Pilot Quantity, Combustion Phasing*  
781 *and EGR on Efficiencies of a Gasoline PPC Light-Duty Engine*. 2017, SAE International.
- 782 37. Blair, G.P., *Design and Simulation of Two-Stroke Engines*. US, 1996.
- 783